

# Thermal conductivity of highly oriented polyethylene

C. L. Choy, W. H. Luk and F. C. Chen

Department of Physics, The Chinese University of Hong Kong, Hong Kong

(Received 22 August 1977; revised 21 September 1977)

We have measured the thermal conductivity of oriented polyethylene both along and perpendicular to the draw direction for draw ratio  $\lambda$  between 1–25 and in the temperature range of 120 to 320K. The results for  $\lambda \leq 5$  have been analysed in terms of the modified Maxwell model while the further increase of thermal conductivity along the draw direction at higher  $\lambda$  has been explained by the Takayanagi model. The Young's modulus and thermal conductivity along the draw direction for the sample with  $\lambda = 25$  were found to be 64 GN/m<sup>2</sup> (at 220K) and 140 mW/cm K (at 300K), respectively, which are extremely high values for polymers. This material, which is a good electrical insulator and yet has a high thermal conductivity, may be useful in electrical applications requiring large dissipation of heat.

## INTRODUCTION

When a semicrystalline polymer is oriented the thermal conductivity along the orientation direction ( $K_{\parallel}$ ) increases rapidly while in the perpendicular direction it ( $K_{\perp}$ ) shows a moderate decrease<sup>1–4</sup>. Physically, this effect can be understood in the following manner. Because the intra-chain covalent bonds are much stronger than the inter-chain van der Waals forces the thermal conductivity of the crystalline regions along the chain direction ( $K_{c\parallel}$ ) is expected to be much larger than that ( $K_{c\perp}$ ) in the perpendicular direction. Since the process of orientation aligns the chains in the crystallites along the draw direction, it causes a rapid increase of the bulk conductivity  $K_{\parallel}$  along the same direction. Similarly, the increase in thermal resistance of the crystallites perpendicular to the draw direction gives rise to a decrease in  $K_{\perp}$ .

A two phase model has recently been proposed<sup>5</sup> to account quantitatively for the orientation effect. It considers an assembly of thermally anisotropic crystallites embedded in an amorphous matrix and takes into account the orientation of the chains with respect to the draw direction. Although the agreement with experiment is quite good at low draw ratio ( $\lambda \leq 5$ ) the model predicts a slow saturation of  $K_{\parallel}$  at higher  $\lambda$ , while the observed  $K_{\parallel}$  shows a continued increase. This has been attributed<sup>3,6</sup> to the increasing importance of the taut tie molecules which provide paths of high thermal conductance between the crystallites along the draw direction. Then the continuing increase of  $K_{\parallel}$  with  $\lambda$  can be understood as the reflection of the increase of the number of tie molecules, and the modified Takayanagi model<sup>7</sup> has been used<sup>3</sup> to put the treatment on a more quantitative basis.

Previous studies of orientation effect have been concentrated mostly on polyethylene (PE)<sup>1–3,8</sup>. Unfortunately, data are available only within a limited temperature range (either at room temperature or below 100K) so that some aspects of the above models have not been tested. We pre-

sent here  $K_{\parallel}$  and  $K_{\perp}$  measurements on PE for  $\lambda = 1$  to 25 between 120 and 320K. The results have been analysed by use of the above two models, which are found to be satisfactory throughout the whole temperature range. For the sample with  $\lambda = 25$ ,  $K_{\parallel}$  is extremely high, varying from 85 mW/cm K at 120K to 140 mW/cm K at 320K, which is comparable to stainless steel<sup>9</sup> over the whole temperature range. The anisotropy  $A \equiv K_{\parallel}/K_{\perp}$  at room temperature is about 60, which is of about the same order of magnitude as the corresponding values for two solids with larger anisotropy arising from layer structures, i.e. pyrolytic graphite ( $A \approx 210$ )<sup>10,11</sup> and boron nitride ( $A \approx 100$ )<sup>12</sup>.

In this experiment the actual measurement was made on thermal diffusivity  $\alpha$ , from which thermal conductivity  $K$  was obtained through the relation  $K = \rho C \alpha$ ,  $\rho$  being the density and  $C$  the specific heat of the polymer. The diffusivity was measured by the flash method originally developed for use on radioactive nuclear fuel elements but recently adapted to polymers<sup>13</sup>. In such a measurement the radiant energy of a flashlight was used to pulse-heat the front surface of a suspended cylindrical sample, and the transient temperature difference between its front and back surfaces as sensed by attached thermocouple junctions was recorded on a potentiometric recorder as a function of time.  $\alpha$  was then deduced from the decay time constant and corrected against effects of radiation loss by a special procedure. For application to oriented polymers in the form of thin sheets it was necessary first to cut them into strips of appropriate size and then bond the strips together into sample cylinders by very thin layers of epoxy resin. While the underlying principle for measuring  $\alpha$  of such samples remains the same as isotropic samples, the procedure for radiation correction must be modified, and the effect of the epoxy on  $\alpha$  must also be assessed. Together with experimental techniques, these are discussed in the next section, where it is shown that only relatively minor modification of our previous work<sup>13</sup> is necessary. The results are analysed (see below) in terms of the modified Maxwell model and the Takayanagi model, with discussions on their physical significance.

Table 1 Summary of data on oriented samples of high density polyethylene

Draw ratio, $\lambda$	$K_{\parallel}$ (mW/cm K)		$K_{\perp}$ (mW/cm K)		Density (gm/cm <sup>3</sup> )	Modulus at 220K (GN/m <sup>2</sup> )	$a'$	$b$
	120K	300K	120K	300K				
1	7.80	5.45	—	—	0.970	—	—	—
2	11.2	10.0	4.90	4.35	0.965	—	—	—
3	15.2	16.1	—	—	0.961	—	—	—
4.5	19.3	23.0	3.90	3.30	0.959	—	—	—
6	26.0	35.3	3.50	2.90	0.965	17	0.202	0.014
10	43.0	65.0	—	—	0.953	28	0.206	0.027
15	63.0	97.0	2.85	2.55	0.955	40	0.209	0.044
25	84.5	138.0	2.80	2.35	0.957	64	0.215	0.070

## EXPERIMENTAL

## Sample preparation and characteristics

The starting material for the samples used is high density PE pellets supplied by British Petroleum Chemicals, Ltd (trade name Rigidex 50), with weight-average and number-average molecular weights equal to 86 800 and 9800, respectively, as determined by gel permeation chromatography<sup>14</sup>. The pellets were compression moulded at 433K into 2.5 mm thick isotropic sheets, which were then slowly cooled at the rate of about 1.5K/min to 383K and then quenched in water at room temperature.

A series of oriented samples were then obtained by rolling the isotropic sheets at room temperature into successively reduced thickness, and the nominal 'draw ratio',  $\lambda$ , defined as the ratio of the final length after rolling to the initial length, gives an indication of the degree of orientation. Five different samples with  $\lambda = 2-4.5$  were produced with hardly any increase in the lateral dimension. Following Capaccio and Ward<sup>15,16</sup>, we obtained a second series of samples by drawing the isotropic sheets on an Instron tensile machine at 348K and at a rate of 5 cm/min, producing a wide range of draw ratio  $\lambda$  from 6 to 25 by using different drawing time.

The density  $\rho$  of the samples shown in Table 1 were determined by the flotation method, using a mixture of toluene and carbon tetrachloride. The volume fraction crystallinity  $X$  of the isotropic sample was found to be 0.80 on the assumption that the density of the crystalline and the amorphous region are 1.000 and 0.855 g/cm<sup>3</sup>, respectively. We assume that the oriented samples have roughly the same crystallinity, since infra-red<sup>17</sup> and wide line n.m.r.<sup>18</sup> studies have indicated a change in  $X$  of less than 10% throughout the range of  $\lambda$ , and, in any case, a similar determination of  $X$  from the density is impractical for the oriented samples because of the production of voids and the possible change of density of the amorphous region due to the drawing process itself.

For determining thermal conductivity,  $K$ , from diffusivity,  $\alpha$ , one also needs the specific heat  $C$  of the samples. On physical grounds orientation is expected to have little effect on  $C$  of crystalline polymers at temperatures well below the melting point. For low draw ratio this has been confirmed by previous studies on other polymers<sup>19</sup>. So we use the published values<sup>20</sup> of  $C$  for isotropic PE for all oriented samples.

For use in actual measurements the oriented PE sheets were first cut into rectangular strips of equal length but varying width; they were then glued together on the flat side by intervening thin films of epoxy resin, so as to form

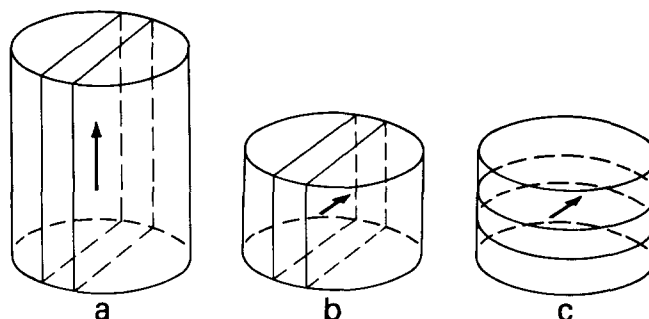


Figure 1 The sample cylinders used for measuring thermal diffusivities  $\alpha_{\parallel}$  (a) and  $\alpha_{\perp}$  (b, c). Within each cylinder one of its component anisotropic rectangular strip or circular disc is shown together with the draw direction (denoted by an arrow) to indicate the relative directions. Heat flow is along the cylindrical axis

roughly a right circular cylinder, with the draw direction  $\hat{n}$  of the polymer strips either parallel or perpendicular to the cylindrical axis (Figure 1), for the measurement of  $\alpha_{\parallel}$  (diffusivity along  $\hat{n}$ ) and  $\alpha_{\perp}$  (diffusivity normal to  $\hat{n}$ ), respectively. Weighing shows that epoxy accounts for about 1–3% of the cylinder mass and, since the density of epoxy is about the same as that of PE, this means the thickness of the epoxy film is also 1–3% of that of the PE strips. The diameter of the sample cylinder varies between 6–12 mm (thus each containing about 10–15 PE strips of 0.5–1.2 mm thickness) and its length was adjusted to produce a thermal relaxation time of 3–15 sec, thus varying between 6–30 mm for the cylinders used for measuring  $\alpha_{\parallel}$  and between 4–6 mm for those used for measuring  $\alpha_{\perp}$ . For the measurement of  $\alpha_{\perp}$  it is also possible to make the sample cylinder by an alternative method, i.e. cutting circular discs from the oriented sample sheets and then gluing them in a stack (Figure 1c). We have made a few measurements at low  $\lambda$  using this alternative arrangement, and found that the results agree with those obtained from the standard arrangement to within experimental accuracy, thus checking that the sample sheet is isotropic in directions normal to  $\hat{n}$ .

## Method of measurement

A number of authors<sup>13,21,22</sup> have shown that if the front surface of an isotropic cylinder of length  $L$  and thermal diffusivity  $\alpha$  is exposed to a very short pulse of flash light then the transient temperature difference  $\theta(t)$  between the front and the back surface is, if radiation loss is neglected:

$$\theta(t) = \theta_0 \sum_{m=1,3,\dots} \exp(-m^2 t/t_c) \quad (1)$$

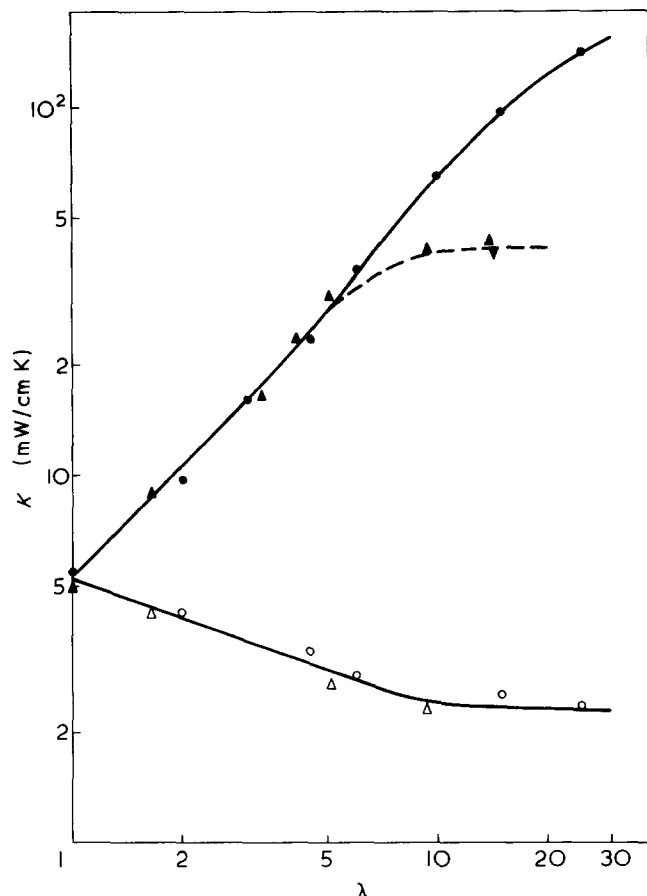


Figure 2 Variation of the thermal conductivity of PE at 300K with draw ratio. Our data for rolled ( $\lambda < 5$ ) and drawn ( $\lambda > 5$ ) samples: ●,  $K_{\parallel}$ ; ○,  $K_{\perp}$ . Data of Hansen and Bernier<sup>1</sup>: ▲,  $K_{\parallel}$ ; △,  $K_{\perp}$ , for sheared samples. ▼,  $K_{\parallel}$  for a sample drawn at 125°C

where  $\theta_0$  is a constant and  $t_c$  is the following characteristic time constant of the sample:

$$t_c = \frac{L^2}{\pi^2 \alpha} \quad (2)$$

Clearly, at relatively large  $t$  ( $> 0.6t_c$ , say)  $\theta(t)$  behaves simply like an exponential decay curve with time constant  $t_c$ , from which  $\alpha$  could be determined. This is the basis of the flash method<sup>13,20,21</sup> for measuring the diffusivity of an isotropic sample.

If the material is thermally anisotropic but with a symmetry axis  $\hat{n}$  either parallel or normal to the front surface the direction of heat flow would still be along the cylindrical axis  $\hat{z}$ , and equations (1) and (2) remain valid, except that one would get two different characteristic time constants  $t_c$ , depending on whether the sample is made for  $\hat{n}$  parallel or perpendicular to  $\hat{z}$ , thus leading to the two different diffusivities  $\alpha_{\parallel}$  and  $\alpha_{\perp}$ , respectively.

However, the thermal anisotropy of the cylinder and the fact that it is made of thin strips glued together by epoxy do imply that one might need a different procedure in correcting for radiation loss. We have investigated the mathematical formalism required for such a correction in some detail in the Appendices, and found that a satisfactory (but slightly more involved) procedure analogous to the one previously used for isotropic samples does exist. However, in this particular experiment the PE sample has a relatively high thermal conductivity, such that the effect of radiation

loss is quite small. In fact radiation loss is less than 1% at 120K and does not exceed 10% even at the highest temperature. Under such circumstances it turns out (see Appendix I) that hardly any significant difference in the correction factor is made by the sample anisotropy, and one can in effect apply the previous (simpler) correction procedure\* without change. In addition the presence of the epoxy used for gluing has the effect of lengthening the thermal relaxation time  $t_c$  by only 1–3%, which is mainly determined by the ratio of the thickness of the epoxy to that of the polymer strip (Appendix II). We therefore shall not go into further details of these small corrections, and refer the reader to the Appendices for the formulae used and for a general discussion on the effects to be expected in various situations.

After all the corrections have been made, we estimate that the data have about the same overall precision (3%) and accuracy (10%) as before<sup>13</sup>.

#### Measurement of Young's modulus

The data are analysed in the Takayanagi model, which predicts increases in both the thermal conductivity and Young's modulus along the draw direction with increasing  $\lambda$ . We have therefore also measured  $E_{\parallel}$  of the drawn samples at 220K and at a frequency of 10 Hz using a forced vibration type equipment manufactured by Iwamoto Seisakusho, Ltd. The accuracy is estimated to be about 15%.

## RESULTS AND DISCUSSION

### General features

The data of thermal conductivity and modulus are summarized in Table 1; the draw ratio and temperature dependence of  $K_{\parallel}$  and  $K_{\perp}$  are also shown in Figures 2 and 3. From Figure 2 it is apparent that for  $\lambda \leq 6$  samples prepared from three different methods of orientation, namely, rolling at room temperature, drawing at 348K and simple shearing at 338K all follow the same  $K_{\parallel}$  versus  $\lambda$  curve, thus implying a unique relationship between  $K_{\parallel}$  and  $\lambda$  irrespective of deformation processes. However, at higher  $\lambda$ ,  $K_{\parallel}$  becomes sensitive to the deformation process, and our samples prepared according to the procedure of Ward and Capaccio<sup>15</sup> (i.e. drawing at 5 cm/min and at 348K) have  $K_{\parallel}$  values much larger than the results obtained by Hansen and Bernier<sup>1</sup> on samples produced either by simple shear or by drawing at 398K. This difference could probably be attributed to the fact that the first drawing process leads to the production of more taut tie molecules, which provide effective thermal paths along the draw direction. The accompanying increase of  $E_{\parallel}$  with  $\lambda$  (see Table 1) is also consistent with this conjecture. On the other hand, the tie molecules are not expected to have much effect on  $K_{\perp}$ , which has essentially the same  $\lambda$  dependence for all samples, irrespective of the deformation processes (Figure 2).

Figure 3 shows that the slopes of the  $K_{\parallel}$  versus temperature curves change gradually from negative to positive as  $\lambda$  increases from 1 to 25, whereas all  $K_{\perp}$  curves have negative slopes. Our  $K_{\parallel}$  data at the low temperature end and the  $E_{\parallel}$  data at 220K (see Table 1) agreed to within 20% with previous results obtained on rods extruded at 373K<sup>3</sup>, implying that these two deformation processes are quite similar as far as

\* The graph of the correction factor previously published<sup>13</sup> is in error for relatively flat cylinders. Compare Figure A1 and Figure 1 of ref 13.

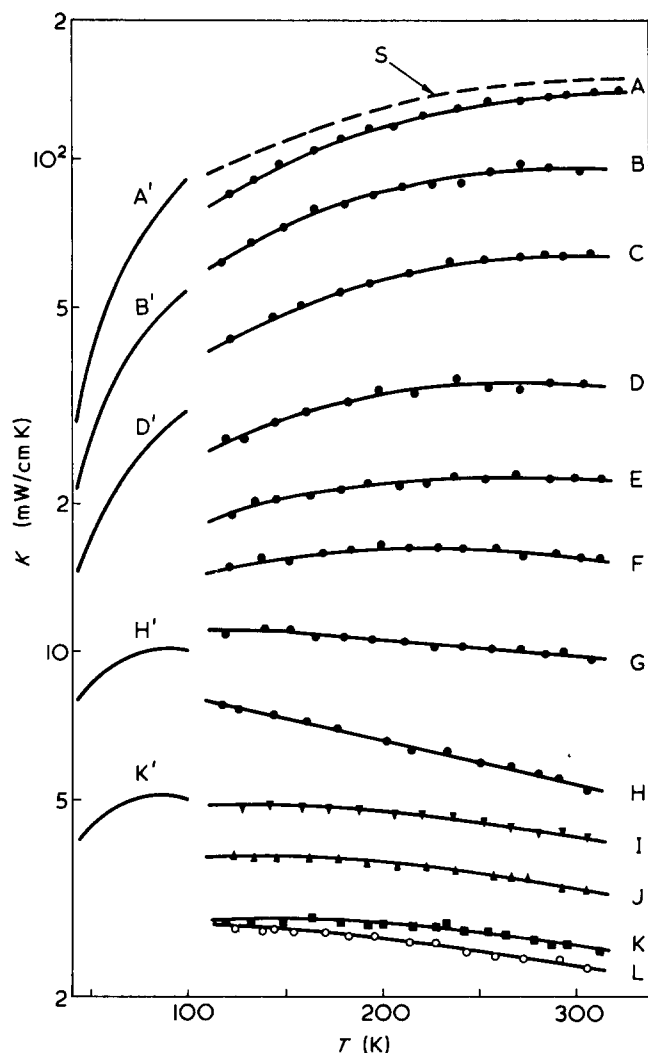


Figure 3 Variation of the thermal conductivity of PE with temperature. Our data for PE,  $K_{\parallel}$ : A,  $\lambda = 25$ ; B,  $\lambda = 15$ ; C,  $\lambda = 10$ ; D,  $\lambda = 6$ ; E,  $\lambda = 4.5$ ; F,  $\lambda = 3$ ; G,  $\lambda = 2$ ; H,  $\lambda = 1$ .  $K_{\perp}$ : I,  $\lambda = 2$ ; J,  $\lambda = 4.5$ ; K,  $\lambda = 15$ ; L,  $\lambda = 25$ . Data of Gibson *et al.*<sup>3</sup> on extruded samples,  $K_{\parallel}$ : A',  $\lambda = 25$ ; B',  $\lambda = 13$ ; D',  $\lambda = 5.4$ ; H',  $\lambda = 1$ .  $K_{\perp}$ : K',  $\lambda = 5.4-25$ . S: data for stainless steel

the production of taut tie molecules are concerned. However, the  $K_{\perp}$  data on extruded rods<sup>3</sup> show saturation above  $\lambda = 5$ , while our data continue to decrease for  $\lambda$  up to 15, at which they are more than 40% lower than the previous results. This could be the consequence of some slight difference in the structure of the two series of samples.

#### Modified Maxwell model

The data at low draw ratio ( $\lambda \leq 5$ ) can best be understood in the modified Maxwell model proposed by Choy and Young<sup>5</sup>. In this model a semicrystalline polymer is treated as an ensemble of spherical crystallites (which approximate the nearly cubical mosaic crystalline blocks) of thermal conductivities  $K_{c\parallel}$  and  $K_{c\perp}$  (along and normal to the chain axis  $\hat{c}$ , respectively) embedded in an amorphous medium with isotropic thermal conductivity  $K_a$ . While  $\hat{c}$  is distributed at random in the isotropic sample, the process of orientation produces a strongly preferred distribution in the angle  $\theta$  between  $\hat{c}$  and the draw direction  $\hat{n}$ , which can be characterized by either  $\langle \cos^2 \theta \rangle$  (the angled bracket indicates averaging over all crystallites) or the crystalline orientation function  $f_c$ :

$$f_c = \frac{1}{2} [3\langle \cos^2 \theta \rangle - 1] \quad (3)$$

which varies between 0 for random orientation and 1 for full orientation of  $\hat{c}$ . As for the thermal conductivity of the amorphous phase, one expects it to be comparable in magnitude to  $K_{c\perp}$  but much smaller than  $K_{c\parallel}$  ( $K_a \approx K_{c\perp} \ll K_{c\parallel}$ ) on physical grounds. There is also sufficient evidence to support the assumption that it remains roughly isotropic and unchanged in magnitude by the orientation process. Under these conditions (which are discussed in detail in refs 5 and 6) the model predicts the following thermal conductivities  $K_{\perp}$  and  $K_{\parallel}$  (normal to and along the draw direction, respectively) for the oriented semicrystalline polymer:

$$\frac{K_{\perp} - K_a}{K_{\perp} + 2K_a} = \frac{X[2k_{\perp} + 1 - 3\langle \cos^2 \theta \rangle]}{2(k_{\perp} + 2)} \quad (4)$$

$$\frac{K_{\parallel} - K_a}{K_{\parallel} + 2K_a} = \frac{X[k_{\perp} - 1 + 3\langle \cos^2 \theta \rangle]}{k_{\perp} + 2} \quad (5)$$

where  $k_{\perp} = K_{c\perp}/K_a$  and  $X$  is the volume fraction of the crystallites, i.e. the crystallinity. In the case of the isotropic sample  $\langle \cos^2 \theta \rangle = 1/3$  and its conductivity  $K_i$  is given by the following reduced form of either equation (4) or (5):

$$K_i = K_a \left[ 1 + \frac{3Xk_{\perp}}{2 + (1 - X)k_{\perp}} \right] \quad (6)$$

We note that the above results are independent of  $K_{c\parallel}$ , which is so large that its effect has already been saturated. As previously discussed<sup>5,6</sup> the thermal conductivity for all amorphous polymers have essentially the same magnitude and temperature dependence, so  $K_a$  for PE has been estimated<sup>5,6</sup> to within 10% by extrapolating the thermal conductivity of its melt down to lower temperature.  $K_{c\perp}$  has also been determined<sup>5,6</sup> from data on isotropic samples by fitting equation (6) to the  $K_i$  versus  $X$  curves, and, along with  $K_a$ , are shown as functions of temperature in Figure 4. The orientation function  $f_c$  (or, equivalently,  $\langle \cos^2 \theta \rangle$ ) for drawn PE (with  $X \approx 0.8$ ) is available in literature<sup>23</sup>, and is used in our analysis of both the drawn and rolled samples. This is reasonable, since it is known that  $f_c$  has similar  $\lambda$ -dependence for a great variety of drawn polymers<sup>23,24</sup>, and that rolled PE exhibits a  $\hat{c}$  distribution similar to that of drawn PE despite its double orientation texture<sup>25</sup>. This is also consistent with the fact that for  $\lambda \leq 6$ ,  $K_{\parallel}$  and  $K_{\perp}$  are insensitive to the different kinds of deformation processes, as revealed in Figure 2.

Thus all parameters appearing on the right of equations (4)–(6), i.e.  $X$ ,  $k_{\perp}$  and  $\langle \cos^2 \theta \rangle$ , can be physically determined, and it is possible to calculate  $K_i$ ,  $K_{\parallel}$  and  $K_{\perp}$  from these equations without the use of any free parameters. The results of calculation are compared with data in Figure 4, which shows that there is satisfactory agreement (within 10%, say) between the two for  $K_i$  and  $K_{\parallel}$  over the entire temperature range of 120 to 320K. The temperature dependence of these two conductivities can be readily understood from the fact that  $K_{c\perp}$  has a large negative temperature coefficient whereas that for  $K_a$  is small and positive<sup>5,6</sup>.  $K_i$  depends on both  $K_a$  and  $K_{c\perp}$  [equation (6)], but the stronger temperature dependence of the latter dominates, and so  $dK_i/dT < 0$ . As  $f_c$  increases, the crystalline axis  $\hat{c}$  becomes aligned with the draw direction  $\hat{n}$ , such that  $K_{c\perp}$

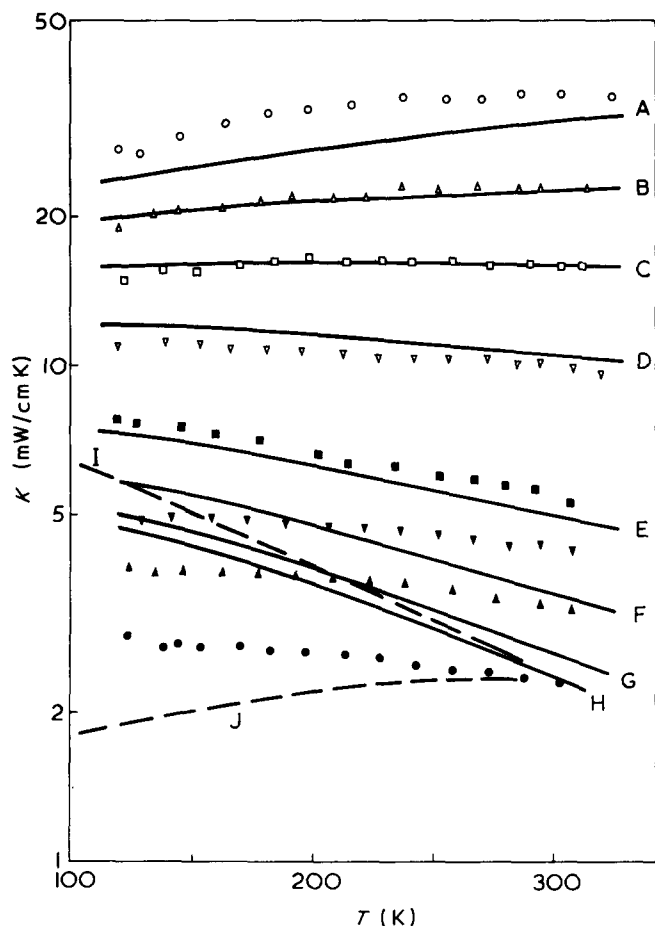


**Figure 4** Comparison of the observed thermal conductivity of PE with the prediction of the modified Maxwell model,  $K_{||}$  data:  $\circ$ ,  $\lambda = 6$  ( $f_c = 0.94$ );  $\triangle$ ,  $\lambda = 4.5$  ( $f_c = 0.88$ );  $\square$ ,  $\lambda = 3$  ( $f_c = 0.73$ );  $\nabla$ ,  $\lambda = 2$  ( $f_c = 0.50$ );  $\blacksquare$ ,  $\lambda = 1$  ( $f_c = 0$ ).  $K_{\perp}$  data:  $\nabla$ ,  $\lambda = 2$  ( $f_c = 0.50$ );  $\blacktriangle$ ,  $\lambda = 4.5$  ( $f_c = 0.88$ );  $\bullet$ ,  $\lambda = 25$  ( $f_c \approx 1$ ). Theoretical predictions according to equations (4)–(6),  $K_{||}$ : A,  $f_c = 1$ ; B,  $f_c = 0.88$ ; C,  $f_c = 0.73$ ; D,  $f_c = 0.50$ ; E,  $f_c = 0$ .  $K_{\perp}$ : F,  $f_c = 0.50$ ; G,  $f_c = 0.88$ ; H,  $f_c = 1$ . I and J are  $K_{c\perp}$  and  $K_a$ , respectively

contributes less and less to  $K_{||}$ , which thus becomes dominated by  $K_a$  and changes to an increasingly positive slope in temperature, until, at  $f_c = 1$ , it equals  $K_a(1 + 2X)/(1 - X)$ , i.e. is proportional to  $K_a$ .

The results are less satisfactory for  $K_{\perp}$ : although there is good agreement at 200K, it is quite apparent that the model predicts much too large a temperature dependence, so the discrepancy between calculation and data rises to about 20% at both ends of the temperature range.

At yet higher draw ratios ( $\lambda \geq 6$ ) the model breaks down, as could be seen from the  $K_{||}$  data for  $\lambda = 6$  ( $f_c = 0.94$ ), which already exceed the model calculation for fully oriented crystallites ( $f_c = 1$ ) by 10% (Figure 4); at the highest draw ratio ( $\lambda = 25$ )  $K_{||}$  is more than 4 times the model prediction (cf Figures 3 and 4). So it is quite obvious that at  $\lambda \geq 6$  the deformation process produces not just crystallite orientation but also morphological changes which are beyond the scope of the modified Maxwell model.

#### Takayanagi model

The nature of the morphological changes caused by large scale ( $\lambda > 5$ ) deformation has received a great deal of attention. It is now established<sup>26</sup> that the spherulitic structure of a semicrystalline polymer is completely destroyed by the process and each lamella is fractured into many smaller crystalline blocks which alternate with the amor-

phous region along the draw direction. Moreover, a large number of taut tie molecules originating from partial chain unfolding now form intercrystalline bridges of extremely high thermal conductance and mechanical strength. This provides a natural explanation for the marked and continued increase of  $K_{||}$  and  $E_{||}$  with  $\lambda$ , but is not expected to have a drastic effect on  $K_{\perp}$ , for which there is indeed no great disagreement between data and the prediction of the modified Maxwell model up to  $\lambda = 25$  (see Figure 4).

The Takayanagi model provides a crude description of this situation. The amorphous region is conceived as a block of length  $a'$  and width  $1 - b$ , in parallel with another block (the intercrystalline bridges) of equal length and width  $b$ , while the combination is in series with the crystalline region, which is of length  $1 - a'$  and width 1 (Figure 5). Previous work<sup>3</sup> shows that for a sufficiently oriented polymer the intercrystalline bridges (which are assumed to possess the same high thermal conductivity and modulus as the crystallites) dominate the amorphous region in thermal conductance for temperatures above 30K, and also in mechanical modulus in the plateau region near 220K at the frequency of our measurement (10 Hz). In that case it can be easily shown<sup>3</sup> that

$$\frac{K_{||}(T)}{K_{c||}(T)} = \frac{E_{||}(\text{plateau})}{E_{c||}} = \frac{b}{a' + b(1 - a')} \quad (7)$$

Consequently at fixed temperature but for various draw ratio  $K_{||}(T)$  should be proportional to  $E_{||}(\text{plateau})$ , as verified in Figure 6. From the slopes of the plot and the knowledge<sup>27</sup>  $E_{c||} \approx 240 \text{ GN/m}^2$  one can directly deduce  $K_{c||}(T)$ , which turns out to vary from 345 mW/cm K at 120K to 540 mW/cm K at 300K. These are about 200 times  $K_a$ , thus fully justifying our earlier assumption that  $K_{c||} \gg K_a$ .

Furthermore, from the ratio  $K_{||}(T)/K_{c||}(T)$  and the crystallinity  $X = 1 - a'(1 - b) \approx 0.8$  one can also determine the values of  $a$  and  $b$  at each  $\lambda$ .  $a$  is found to remain roughly unchanged at 0.21 while  $b$  increases from 0.014

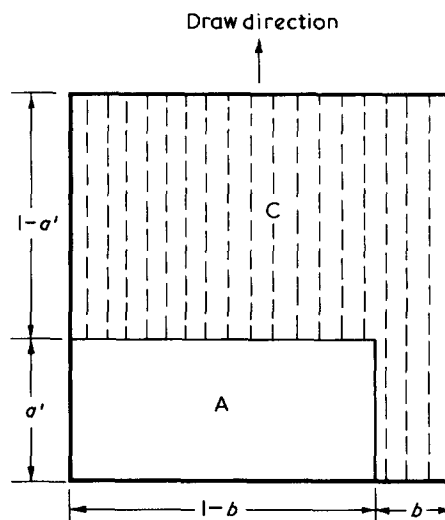


**Figure 5** Schematic representation of the Takayanagi model for a drawn semicrystalline polymer. A and C denote the amorphous and crystalline regions, respectively; (---) represent the chain axes

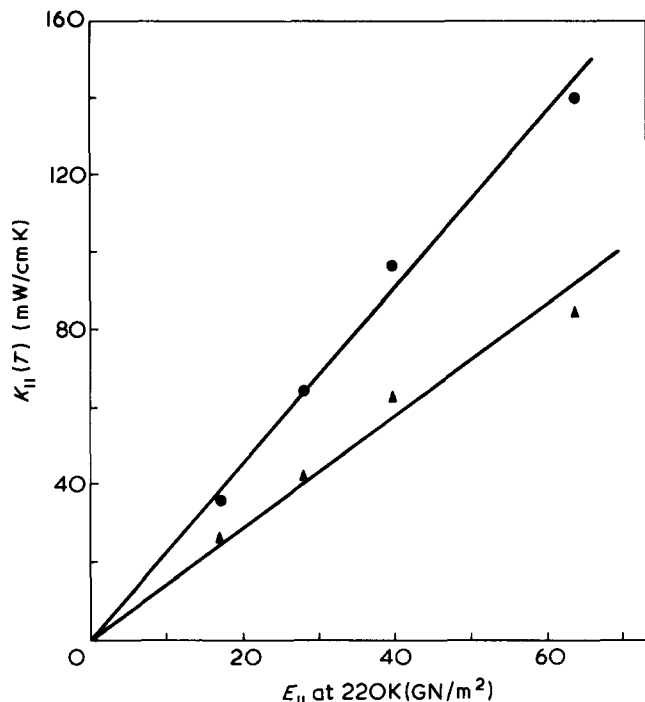


Figure 6 Variation of the thermal conductivity along the draw direction at temperature  $T$  with the Young's modulus in that direction measured at 220K.  $\blacktriangle$ ,  $T = 100\text{K}$ ;  $\bullet$ ,  $T = 300\text{K}$

to 0.070 as  $\lambda$  increases from 6 to 25. These values are consistent with our neglecting the intercrystalline bridges in the modified Maxwell model (for which  $\lambda < 6$ ,  $b < 0.014$ ), and with the assumptions leading to equation (7).

The value of  $K_{C||}(T)$  can also be used for an estimate of the phonon mean free path  $l$  along the chain direction from the expression  $K_{C||} = Cv l$ , where  $C$  is the acoustic specific heat of PE. Closely following the method of the previous work<sup>6</sup>, we find  $l$  to be approximately constant at 75 Å from 120 to 300K, in agreement with an earlier determination for the temperature range of 50 to 100K, thus supporting the view that  $l$  is mainly determined by the geometric dimension of the crystalline blocks in the draw direction, which is of the order of 100–300 Å<sup>26</sup>.

## CONCLUSIONS

We conclude that the modified Maxwell model can satisfactorily account for the thermal conductivity of oriented polyethylene below  $\lambda = 5$  while the further increase of  $K$  at higher  $\lambda$  can be understood within the framework of the Takayanagi model. Since the drawn sample at  $\lambda = 25$  has both high modulus and thermal conductivity along the draw direction it may be useful in industrial applications which require a good electrical insulator also to have a high thermal conductivity to dissipate heat. The common method for improving heat conduction in thermoplastics or epoxy resins is to add a filler of high conductivity such as copper, aluminium, aluminium oxide, etc.<sup>28–31</sup>. However, even with a filler volume fraction of 0.4 the thermal conductivity is enhanced only 4-fold, whereas we have seen that the thermal conductivity of polyethylene can be increased from 5.5 to 140 mW/cm K i.e. 25 times by drawing to  $\lambda = 25$ .

## ACKNOWLEDGEMENTS

We are grateful to Mr G Downs and Mr J. C. H. Scott of BP Chemicals Ltd for kindly supplying the starting material for our work, and to Mr R. Stone of the Engineering Department of Oxford University for help in the preparation of the rolled samples. Thanks are also due to Dr K. Young of the Physics Department of the Chinese University of Hong Kong for reading this article and to Mr O. K. Chan for help in the measurements.

## REFERENCES

- Hansen, D. and Bernier, G. A. *Polym. Eng. Sci.* 1972, 12, 204
- Burgess, S. and Greig, D. *J. Phys. (C)* 1975, 8, 1637
- Gibson, A. G., Greig, D., Sahota, M., Ward, I. M. and Choy, C. L. *J. Polym. Sci. (Polym. Lett. Edn)* 1977, 15, 183
- Choy, C. L. and Greig, D. *J. Phys. (C)* 1977, 10, 169
- Choy, C. L. and Young, K. *Polymer*, 1977, 18, 769
- Choy, C. L. *Polymer* 1977, 18, 984
- Takayanagi, M., Imada, K. and Kajiyama, T. *J. Polym. Sci. (C)* 1966, 15, 263
- Killian, H. G. and Pietralla, M. *Polymer*, submitted for publication
- White, G. K. 'Experimental Techniques in Low Temperature Physics', Clarendon Press, Oxford, 1968, pp 380
- Hooker, C. N., Ubbelohde, A. R. and Young, D. A. *Proc. Roy. Soc. (A)* 1965, 284, 17
- Taylor, R. *Phil. Mag.* 1966, 13, 157
- Simpson, A. and Stuckes, A. D. *J. Phys. (C)* 1971, 4, 1710
- Chen, F. C., Poon, Y. M. and Choy, C. L. *Polymer*, 1977, 18, 129
- Downs, G. personal communication
- Capaccio, G. and Ward, I. M. *Polymer*, 1974, 15, 233
- Capaccio, G., Crompton, T. A. and Ward, I. M. *J. Polym. Sci. (Polym. Phys. Edn)* 1976, 14, 1641
- Glenz, W. and Peterlin, A. *J. Macromol. Sci. (B)* 1970, 4, 473
- Smith, J. B., Manuel, A. J. and Ward, I. M. *Polymer* 1975, 16, 57
- See, for example: Dole, M., Hettinger, W. P., Larson, N. and Wethington, J. A. *J. Chem. Phys.* 1952, 20, 37; Smith, C. W. and Dole, M. *J. Polym. Sci.* 1956, 20, 37
- Chang, S. S. and Bestul, A. B. *J. Chem. Phys.* 1972, 56, 503
- Parker, W. J., Jenkins, R. J., Butler, C. P. and Abbott, G. L. *J. Appl. Phys.* 1961, 32, 1679
- Cape, J. A. and Lehman, G. W. *J. Appl. Phys.* 1963, 34, 1909
- Pietralla, M. *Kolloid Z. Z. Polym.* 1976, 254, 249
- Samuels, R. J. 'Structured Polymer Properties', Wiley, New York, 1974
- Lin, L. S., Chou, Y. T. and Hu, H. J. *J. Polym. Sci. (Polym. Phys. Edn)* 1975, 13, 1659
- Peterlin, A. *Kolloid Z. Z. Polym.* 1969, 233, 857
- Frank, F. C. *Proc. Roy. Soc. (London) (A)* 1975, 319, 127
- Sundstrom, D. W. and Lee, Y. D. *J. Appl. Polym. Sci.* 1972, 16, 3159
- Garret, K. W. and Rosenberg, H. M. *J. Phys. (D)* 1974, 7, 1247
- de Araujo, F. F. T. and Rosenberg, H. M. *J. Phys. (D)* 1976, 9, 665
- Nieberlein, V. A. and Steverding, B. *J. Mater. Sci.* 1977, 12, 1685

## APPENDIX I

### Radiative loss of an anisotropic cylinder

Our previous procedure<sup>13</sup> for computing  $\alpha$  in the presence of radiation loss from the exponential decay time constant of the front-back temperature difference of a sample was based on the work of Cape and Lehman<sup>22</sup>. We now extend the same approach to an anisotropic cylindrical sample of length  $L$ , radius  $R$ , density  $\rho$ , specific heat  $C$ , thermal conductivity  $K_z$  along the cylindrical axis  $z$  and  $K_r$  perpendicular to  $z$ . For such a sample the equation of

diffusion for temperature  $\theta$  (the ambient temperature being taken as reference) and the boundary conditions for linearized radiative loss are:

$$K_z \partial_z^2 \theta + K_r (\partial_x^2 + \partial_y^2) \theta = \rho C \partial_t \theta \quad (\text{A1})$$

$$\partial_r \theta = -\nu_r \theta \quad r = R \quad (\text{A2})$$

$$\partial_z \theta = -n \nu_z \theta \quad z = 0, L \quad (\text{A3})$$

where  $n = +1$  and  $-1$  at the back ( $z = L$ ) and front ( $z = 0$ ) end of the cylinder, respectively. The constants  $\nu_{r,z}$  are:

$$\nu_{r,z} = \frac{4\sigma e_{r,z} T_0^3}{K_{r,z}} \quad (\text{A4})$$

where  $\sigma$  is the Stefan-Boltzmann constant,  $T_0$  is the absolute ambient temperature and  $e_{r,z}$  is the emissivity for the curved ( $r$ ) and flat ( $z$ ) surfaces of the cylinder.

Make the coordinate transformation  $x = x'/a^{1/2}$ ,  $y = y'/a^{1/2}$  [hence  $r = (x^2 + y^2)^{1/2} = r'/a^{1/2}$ ] and  $z = z'$ , where the scale factor  $a$  is  $K_z/K_r$ . Then equation (1) becomes:

$$K_z \nabla'^2 \theta = \rho C \partial_t \theta \quad (\text{A5})$$

which is appropriate for an isotropic solid of conductivity  $K_z$ . The boundary  $r = R$  changes to  $r' = R' = (a)^{1/2}R$  while the boundaries at  $z = z' = 0$  and  $L$  remain unchanged. If we make the further transformation  $e_r \rightarrow e_r' = (a)^{1/2}e_r$  and  $e_z = e_z'$  then equations (A2)–(A4) become the appropriate boundary conditions for an isotropic cylinder of length  $L$ , radius  $R'$ , conductivity  $K_z$  and emissivities  $e_r'$  and  $e_z'$ . The previous results<sup>13,22</sup> for an isotropic cylinder which has been flash-heated at the front end can therefore be applied directly to this problem, leading to the following expression for  $\theta_{FB}$ , the temperature difference between the centre points of the front and back end surfaces of the cylinder:

$$\theta_{FB}(t) = \sum_{m \text{ odd}} B_m \exp(-\omega_m t/t_c) \quad (\text{A6})$$

where  $B_m$  are coefficients of comparable magnitude and need not concern us here;  $t_c$  is related to the diffusivity  $\alpha_z (=K_z/\rho C)$  along the  $z$ -axis by  $t_c = L^2/\pi^2 \alpha_z$ , and  $\omega_m (m = 0, 1, 2, \dots)$  is:

$$\omega_m = \frac{1}{\pi^2} \left[ x_m^2 + \frac{1}{a} \left( \frac{L}{R} \right)^2 q^2 \right] \quad (\text{A7})$$

where  $x_m$  is the  $m$ th root ( $m = 0, 1, 2, \dots$ ) of

$$\tan x_m = \frac{2yx_m}{x_m^2 - y^2} \quad (\text{A8})$$

and  $q$  is the first root of

$$qJ_1(q) = a \frac{R}{L} yJ_0(q) \quad (\text{A9})$$

where  $J_n(q)$  are Bessel functions of  $n$ th order and  $y = \nu_z L$  is a constant characterizing radiation loss. We note that the dominant decay time of  $\theta_{FB}$  is  $\tau_1 = t_c/\omega_1$ , while the decay time of the entire sample due to radiation loss is  $\tau_0 = t_c/\omega_0$ ,

both of which can be directly measured<sup>13</sup>. Clearly if  $R/L$ ,  $a$  (which can be roughly estimated if radiation loss is neglected), and  $\mu = \omega_0/\omega_1 = \tau_1/\tau_0$  are known then one can solve the implicit equations (A7), (A8) and (A9) numerically to find the correction factor  $\omega_1^{-1}$ , which then allows us to deduce the corrected value of  $\alpha_z$  from the observed decay time constant  $\tau_1$ .  $\omega_1^{-1}$  as a function of  $\mu$  for various values of  $a$  and  $R/L$  is plotted in Figure A1, where it is seen that  $\omega_1^{-1}$  deviates from its corresponding value for the isotropic case ( $a = 1$ ) only when  $a \gg 1$ ,  $\mu$  is relatively large and  $R/L \sim 1$ . This is quite important, since experimentally one can only make a rough estimate of  $a$  when making the correction.

In this experiment the above procedure can be directly applied to the  $\alpha_{\parallel}$  sample, with  $a = A (=K_{\parallel}/K_{\perp} \sim \tau_{1\perp}/\tau_{1\parallel})$ , where  $\perp$  and  $\parallel$  refer to cases in which the draw direction is perpendicular or parallel to the symmetry axis, respectively, but would need further modification for the  $\alpha_{\perp}$  sample, which is not isotropic in the  $xy$  plane. Fortunately  $\mu < 4\%$  for all of our runs, so that one can simply ignore the anisotropy in the  $xy$  plane (which amounts to uncertainty in the value of  $a$ ), whether caused by the arrangement of the polymer strips or by the presence of glue.

## APPENDIX II

### An estimate of the glue effect

Consider heat flow in an infinite stack of polymer strips of length  $L$  and thickness  $2a$  interspersed by uniform layers of glue (epoxy resin) of the same length but thickness  $2b$  ( $b \ll a$ ). The conductivity of the polymer is  $K_z$  along the strip and  $K_x$  across it, while that of the glue is  $K_1$ . It is assumed that the temperature distribution is always uniform

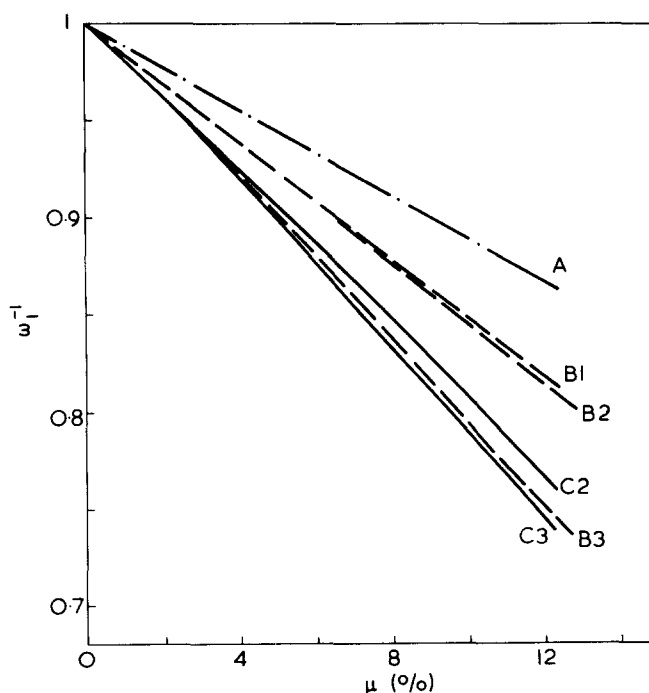


Figure A1 A plot of  $\omega_1^{-1}$  against  $\mu$  for various values of  $R/L$  and anisotropy  $a$ . A,  $R/L = 0.1$ ,  $a = 0.01, 1, 100$ ; B1,  $R/L = 1$ ,  $a = 0.01$ ; B2,  $R/L = 1$ ,  $a = 1$ ; B3,  $R/L = 1$ ,  $a = 100$ . C2,  $R/L = 4$ ,  $a = 0.01$ ,  $a = 1$ ; C3,  $R/L = 4$ ,  $a = 100$

along the  $y$  direction. If a spatially uniform heat pulse is applied to such a stack at  $z = 0$  then by the standard technique of separation of variables the subsequent temperature  $\theta_1$  in the polymer and  $\theta_2$  in the glue are:

$$\theta_1 = \sum_{m,n} A_{mn} \cosh \frac{\gamma_{mn} x}{a} \cos \frac{n\pi z}{L} \exp(-\omega_{mn} t) \quad (\text{B1})$$

$$\theta_2 = \sum_{m,n} B_{mn} \cos \frac{\beta_{mn}(a+b-x)}{b} \cos \frac{n\pi z}{L} \exp(-\omega_{mn} t) \quad (\text{B2})$$

where

$$\begin{aligned} \omega_{mn} &= \alpha_z \left( \frac{n\pi}{L} \right)^2 - \alpha_x \left( \frac{\gamma_{mn}}{a} \right)^2 \\ &= \alpha_1 \left[ \left( \frac{n\pi}{L} \right)^2 + \left( \frac{\beta_{mn}}{b} \right)^2 \right] \end{aligned} \quad (\text{B3})$$

and

$$\alpha_{x,z} = K_{x,z} / \rho_2 C_2$$

$$\alpha_1 = K_1 / \rho_1 C_1$$

are the diffusivities of the polymer and of the glue, respectively.  $\rho_i$  and  $C_i$  are the density and specific heat for the glue ( $i = 1$ ) and polymer ( $i = 2$ ), respectively.

This solution satisfies the equations of diffusion (which is anisotropic in the polymer) and the boundary condition of no heat loss:  $\partial_z \theta = 0$  at  $z = 0$  and  $L$ . Possible  $\sinh \gamma x/a$  and  $\sin \beta x/b$  terms are excluded by the condition of symmetry  $\theta(x) = \theta(-x)$ . Choosing the hyperbolic cosine function for  $\theta_1$  and the cosine function of  $\theta_2$  in  $x$  has the effect of making  $\omega_{mn}$  lower than its corresponding value  $\omega_{0n} = \alpha_z (n\pi/L)^2$  for an infinite medium of diffusivity  $\alpha_z$  but higher than  $\alpha_1 (n\pi/L)^2$ , which is characteristic of glue. That is, the relaxation times would be longer than in polymer but shorter than in glue, as expected physically. We note that the same  $\omega_{mn}$  must appear in both  $\theta_1$  and  $\theta_2$  to make fitting boundary conditions at  $x = \pm a$  possible. These conditions are  $\theta$  and  $J_x = -K \partial_x \theta$  must be continuous at  $x = \pm a$ , leading to (indices  $m$  and  $n$  suppressed):

$$A \cosh \gamma = B \cos \beta \quad (\text{B4})$$

$$K_x \frac{\alpha}{a} A \sinh \gamma = K_1 \frac{B}{b} \sin \beta \quad (\text{B5})$$

So consistency requires

$$\xi \gamma \tanh \gamma = \beta \tan \beta \quad (\text{B6})$$

where  $\xi = K_x b / K_1 a$ . We note that equations (B4) and (B5) also guarantee  $\theta_1(-a) = \theta_2(a + 2b)$  and a similar condition for  $-K \partial_x \theta$ , thus ensuring translational invariance under  $x \rightarrow x + 2n(a + b)$ , as would be expected for an infinite stack.

The transcendental equations (B3) and (B6) determine the eigen values  $\gamma_{mn}$  and  $\beta_{mn}$  and hence also the frequencies  $\omega_{mn}$ . For the parameters characteristic of this experiment it turns out that  $\gamma, \beta \ll 1$ , so equation (B6) is reduced to

$$\xi \gamma^2 = \beta^2 \quad (\text{B7})$$

which, upon substitution into equation (B3) yields the following solution for the characteristic frequency  $\omega_{1m}$ :

$$\begin{aligned} \frac{\omega_{1m}}{\omega_{0m}} - 1 &= - \frac{1 - \eta K_1 / K_z}{1 + \eta a / b} \\ &\rightarrow - \frac{1 - K_1 / K_z}{1 + a / b} \end{aligned} \quad (\text{B8})$$

where the last step assumes approximately equal density and specific heat for the polymer and the glue, such that  $\eta = \rho_2 C_2 / \rho_1 C_1 \rightarrow 1$ .

Clearly the expression on the left of (B8) is simply the negative fractional change in relaxation time  $\tau_{1m} (\equiv 1/\omega_{1m})$ . In case  $K_z \gg K_1$  and  $a \gg b$  such as typical of this experiment we therefore have  $\Delta \tau_{1m} / \tau_{1m} \approx b/a \approx 1-3\%$ . Furthermore, this calculation is of course only based on a very crude approximation of the actual physical situation, in which a finite stack of strips of unequal width is involved, but for our purpose there does not seem to be any point for a more accurate determination of such a small effect. It should also be noted that the glue effect as given by equation (B8) causes the same percentage increase to all relaxation times, thus not affecting  $\mu = \omega_{00} / \omega_{01}$  (Appendix I). It is therefore reasonable to treat radiation loss and the presence of glue as two separate effects without mutual interaction.